

## High pressure experiments for Astrophysics.

P.LOUBEYRE

*Laboratoire PMC, Université Paris 6, boîte 77, 4 place Jussieu 75252 Paris. France.*

### Abstract

In the past decade, measurements of the properties of H<sub>2</sub> and He systems at very high pressures have made great progress, now reaching density at the limit of the plasma phase transition of hydrogen. The potentialities and limits of static and dynamic methods will be reviewed. Then, a survey of the major experimental results is presented. It is the intention of this article to show how these measurements can bring information to model low-mass astrophysical objects. Three levels of usefulness are distinguished on selected examples: data for codes of planetary interiors, constraints for theoretical descriptions of dense matter, observations of unsuspected properties at very high density.

## Abstract

De grands progrès ont été faits ces dix dernières années dans la mesure des propriétés des systèmes d'H<sub>2</sub> et d'He sous très fortes pressions. Des densités à la limite de la transition de phase plasma de l'hydrogène peuvent maintenant être obtenues en laboratoire. Les possibilités et limites des méthodes dynamiques et statiques seront tout d'abord discutées. Ensuite, les principaux résultats expérimentaux seront présentés. Le but de cet article est de montrer comment ces études peuvent être utiles à la modélisation des intérieurs planétaires. Trois niveaux d'application seront dégagés: données pour les codes de structures internes; contraintes pour valider les descriptions théoriques; mise en évidence à très haute densité de comportements inhabituels .

### 11.1 Introduction

The properties of matter at very high density are central to our understanding of planetary interiors. Reliable calculations are difficult, even for the two simplest elements hydrogen and helium. On the other hand, high pressure properties are measured in laboratory by static and dynamic methods. Are these experiments useful for the models of interiors of low-mass astrophysical objects?

The importance of high pressure experiments is fully acknowledged in geophysics (Manghani 1987). Remarkably, measurements of geophysical compounds can now be made under conditions that simulate those found within the deep interior of earth (believed to be close to 350 GPa and 6000 K). In doing so, important issues can be set, such as the melting curve of iron that constrains the temperature of the core (Jeanloz 1990).

In contrast, high pressure measurements are generally considered weakly relevant for astrophysics. Certainly, the PT conditions at the centre of giant planets are far from experimental reach. However, in the past decade few laboratories have been very active in measuring the properties of H<sub>2</sub> and He at very high pressures. In ten years a factor of 100 has been achieved in the maximum static pressure. Multiple shock-wave measurements have been also performed on H<sub>2</sub> and He. Now, the properties of these systems can be measured up to densities at the limit of the plasma phase transition of hydrogen. It is the intention of this article to show how these measurements can give information to model giant planets and brown dwarfs.

This article is organized into three major sections. In section 2, the potentialities and the limits of dynamic and of static methods will be presented and compared. Section 3 is a survey of the recent measurements of the properties of hydrogen and helium at very high pressures. The search for metal hydrogen, that has been the focus of a great activity, will be discussed in details. In section 4, three levels of usefulness for astrophysics are presented with selected examples, namely:

Input data for codes of planetary interiors.

Test for calculations of astrophysical matter.

Observation of unsuspected properties at very high density.

Finally, an outlook of this rapidly growing field will be tentatively given.

## 11.2 *Experimental methods*

Experiments on systems of hydrogen and helium at very high pressures present the maximum difficulties. A conjunction of three factors makes their compression and characterization difficult:

*A very high compressibility.* The volume of the initial state in static or dynamic methods (almost equal to the one of the low temperature liquid at ambient pressure) has to be reduced by a factor 10 and 15, respectively in hydrogen and in helium so as to reach 100 GPa. In dynamic studies, this causes a large increase of temperature along the Hugoniot that prevents compression further. In static studies, this is associated with a large deformation of the sample chamber, lessening its rigidity.

*Low optical tensor.* Various optical techniques are used to characterize systems at very high pressures: X ray diffraction, Raman diffusion, infrared absorption... Because the impinging light acts on the electronic density, optical tensors are weak for these low Z elements. Methods of investigation have to be specially adapted, such as the single crystal x ray diffraction with a synchrotron source (Mao 1988).

*Reactivity of hydrogen.* Due to hydrogen embrittlement, special containers have to be used. The reactivity of hydrogen increases with pressure and its confinement at very high pressures is a problem: An attack of the diamond anvils is suspected around 200 GPa.

Due to these difficulties, hydrogen and helium were not the first systems studied under pressure despite their fundamental interest and their importance for astrophysics. Nevertheless, it should be noted that their demanding pressurization has had a feed-back improvement on the high

pressure techniques.

### 11.2.1 Dynamic methods: shock-waves.

Shock-wave research has been developed after world war II, independently in the United States and in Russia. Shock-wave experiments create a disturbance propagating at supersonic speed in a material, preceded by an extremely rapid rise in pressure, density and temperature. Although irreversible, the process is well-understood and can be controlled to produce a desired response, as reviewed elsewhere (Zeldovich and Raizer 1966, Ross 1985). The measurement of two dynamic variables, the shock front velocity,  $v_s$ , and the perturbation front velocity,  $v_p$ , is sufficient to determine the thermodynamic state of the compressed system. The pressure, volume and entropy (P, V, E) behind the shock front are related to initial properties and the dynamic variables through the Rankine-Hugoniot equations that expresses conservation of mass, momentum and energy. The shock process is highly irreversible and is accompanied by a large increase in temperature. In He and in  $H_2$ , this limits the compression. The resulting P(V) curve is known as the Hugoniot. The determination of the shock pressure is absolute. A considerable variation in the path of the Hugoniot can be achieved with double or multiple shock experiments for which the primary shock is passed through the sample and reflected from a high impedance anvil. The reflected wave then compresses the already compressed material to a higher pressure. At the same density, the temperatures and pressures along the reflected Hugoniot are much lower than those reached by the single shock and tend toward the isentrope.

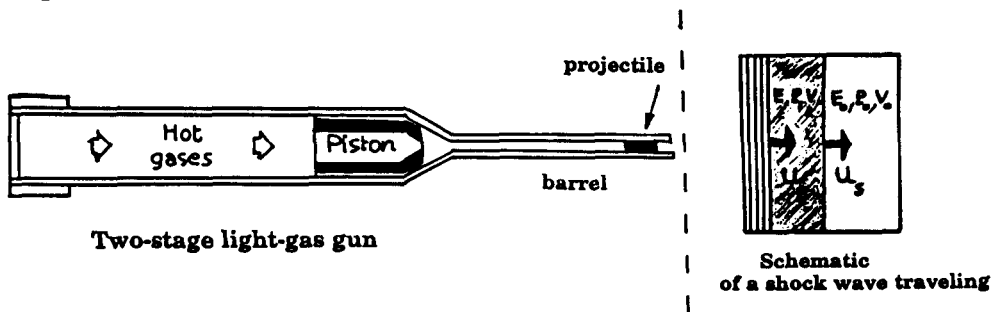


Figure 1: schematic of two-stage light-gas gun and shock-wave traveling.

Shock-wave measurements have been carried out on most elements and on several compounds. Experiments on  $H_2$  and He were all carried at Lawrence Livermore National Laboratory, mostly after 1983. Shock-waves were generated by the impact of a planar projectile into cryogenic specimen holders. Maximum pressures of 21 GPa ( $T \approx 4800$  K), 76 GPa ( $T \approx 7000$  K) and 120 GPa ( $T \approx 3000$  K) have been achieved on liquid  $D_2$

through respectively simple, double and multiple shocks ( Nellis 1983, Weir 1993). Maximum pressures of 16 GPa ( $T \approx 12000$  K) and 56 GPa ( $T \approx 21000$  K) have been achieved on He through respectively single and double shocks (Nellis 1984).

Isentropic compression experiments have also been reported on hydrogen at pressures above 100 GPa in a magnetic flux compression device (Hawke 1978). The volume was measured from flash radiograph of the radii of the sample chamber. Pressures and temperatures were then calculated from a magneto-hydrodynamic code. Such experiments have been designed for conductivity measurements at ultra-high pressures. Hydrogen and deuterium have been compressed by this method to density above  $1\text{g/cm}^3$ , where a conducting behaviour was detected. Although higher densities can be achieved by magnetic compression than with impact shock-wave, the characterization of the thermodynamic state and of the physical properties of the sample is unfortunately quite primitive.

### **11.2.2 Static methods. A revolution, the DAC.**

Before 1979, high pressure studies on  $\text{H}_2$  and He were performed in massive apparatuses, technically very demanding, relatively expensive and dangerous to operate. The highest pressures, about 2 GPa, were obtained in the so-called piston-displacement technique. Measurements of the equation of state, melting curve and sound velocity could be done then.

In 1979, for the first time,  $\text{H}_2$  (Mao 1979) and He (Besson 1979) were loaded in a diamond anvil cell (DAC). Their melting point at room temperature was measured respectively at 5.2 GPa and 11.6 GPa. Today, pressures above 200 GPa can be generated on  $\text{H}_2$  and on He in a DAC that can fit into the palm of the hand. The diamond anvil cell was first designed in 1959. In the history of its evolution that spans over a period of 20 years before He and  $\text{H}_2$  could be loaded, important innovations are to be recognized: The introduction of the metal gasket technique for confining fluid sample; The ruby fluorescence technique for the pressure calibration; The bevelling of the diamond flats to reduce the pressure gradients in the stone and to reach the megabar range ( Jayaraman 1983, 1986).

A diamond anvil cell is a mechanical device to push two opposed diamond anvils together. Single crystal diamonds are used as anvils not only because diamond is the hardest material available but also because perfect diamond is transparent to most electromagnetic radiation over a

wide range of wavelengths from far infra-red to  $\gamma$  rays, apart from the window [3.5eV, 8KeV]. As shown in figure 2, a shim of metal (rhenium for use with hydrogen) is compressed between the two flats of the diamond anvils. The centre hole is made by micro-drilling or spark-erosion after pre-indentation of the gasket up to the limit of the plastic flow of the metal shim. A small ruby chip, for use as the pressure gauge, is put in the cylindrical sample chamber before loading. To load sufficient  $H_2$  or He sample in the DAC, cryogenic or high pressure loading are used. Initial densities are roughly equal in both methods but only the latter one can be used for loading mixtures of gases. Most progress in the generation of megabar pressures has resulted from optimizing the distribution of the force, changing the configuration

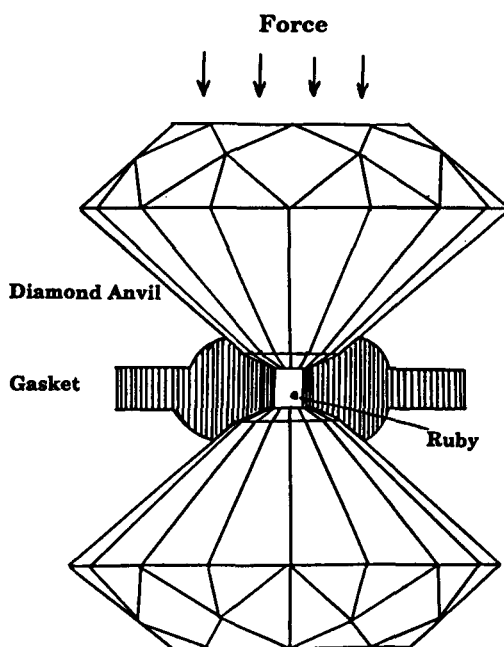


Figure 2: Schematic of the DAC.

of the anvils and achieving high precision of the anvil alignment. There are many designs of DAC, but the recent membrane diamond anvil cell (LeToullec 1988) has appeared to be particularly well-adapted for the studies of dense  $H_2$  and He (axial thrust on diamond, smooth variation of pressure, large optical aperture, easy use in a cryostat,...).

There is a limit to the load that can be exerted on a diamond anvil. Greater pressure is thus generated by reducing the area of the central flat of the diamond tip. Very high pressures are obtained at the expense of smaller volume of the sample. A maximum pressure of 560 GPa, calculated from the volume measured by x ray diffraction, has been reported on Mo and it seems that higher pressures could be generated with the DAC (Ruoff 1992). However, the maximum pressure reported at present on  $H_2$  is around 250 GPa. This is roughly the limit of the ruby pressure gauge which is used for these systems. The pressure shift of the  $R_1$  luminescence band of ruby has been calibrated to 110 GPa by measuring with x ray diffraction the molar volume of copper, gold and tungsten embedded with ruby in the Ne or Ar hydrostatic pressure medium of the DAC sample chamber (Mao 1986). The absolute accuracy of the ruby pressure gauge is estimated to be  $\pm 2\%$ . Various effects render the measurement of pressure by the ruby gauge above 200 GPa almost

impossible: the intensity of the ruby fluorescence decreases markedly with pressure; Stressed diamonds produce a broad luminescence that overwhelms the ruby fluorescence; the closing gap of diamond gives a strong absorption of the laser line; finally, such pressures are far from the range of calibration of the ruby gauge.

Due to the optical transparency of the diamond, the DAC is the tool par excellence for optical spectroscopy at very high pressure: The sample can be fully characterized. Generally, the very weak signals of the minute samples of H<sub>2</sub> and He have to be separated from the strong background of the diamond anvils. Raman, infra-red, absorbance, reflectance, dielectric or Nuclear Magnetic Resonance measurements and single crystal x-ray diffraction of H<sub>2</sub> and He solids had to be adapted. In the next section, the main measurements on H<sub>2</sub> and He systems at high pressure are surveyed.

In table I, we have tried to compare the potentialities, limits and achievements of the dynamic and of the static methods. It seems that the DAC is more suitable for the study of astrophysical matter than the dynamic methods because it combines the generation of higher densities with a full characterization of the sample under static and equilibrium conditions. The coupling of very high temperatures with very high pressures in a DAC, that is being developed, would reinforce this assertion.

*Table 1: Comparison between DAC and Shock-wave for studying H<sub>2</sub> and He systems.*

METHODS	POTENTIALITIES	LIMITS	ACHIEVEMENT
<b>Shock-wave.</b> Single → Hugoniot Reflected → Isentrope	Absolute measurement of P and V No limit of pressure. Conductivity measurement.	Dynamic process. Hard to reach very high density. P(T) curves: Hugoniot, isentrope. Always in the fluid phase. Optical measurements difficult Study of mixtures impossible. Irreversible. Expensive.	D <sub>2</sub> : 120 GPa 3000 K -3.3 cm <sup>3</sup> /mole He: 58 GPa 2100 K -6 cm <sup>3</sup> /mole
<b>Diamond Anvil Cell</b>	Static. X ray measurement of V. Complete optical measurements. Studies of mixtures. Reversible P T path. Low cost, easy use.	Mechanical limit of diamond. Measurement of P < 250GPa. Very small volume. Parasitic properties of diamond No conductivity measurement.	H <sub>2</sub> : 248 GPa 77 K -2.1 cm <sup>3</sup> /mole He: 60 GPa 300 K 2.5 cm <sup>3</sup> /mole

### **11.3 A decade of measurements of the properties of H<sub>2</sub> and He at very high pressures.**

#### **11.3.1 A review of the literature.**

The static studies have been performed essentially by four groups (Geophysical, Harvard, Paris 6 and Van der Waals laboratories). All the shock-wave studies have been performed at Livermore. The present status of their experimental investigations is presented below.

##### **11.3.1.1 Helium.**

He is the simplest atom with a close 1s electronic shell. It has been calculated that the electrons should remain tightly bound to the nucleus up to at least 40 Mbars (Klepeis 1991). Also, due to its very low atomic mass, low density He has been extensively studied as the archetype quantum system. The two following problems have motivated the investigations of the properties of He at very high pressures, namely: How to model the interactions of a dense insulator and in particular what is the validity of a pair potential description? What are the importance of quantum effects at high density?

The melting point at room temperature was the first measurement performed on He in a DAC (Besson 1979). Subsequently, the melting curve measurements were extended up to 24 GPa and 460 K by the method of quasi-isochoric scans (Loubeyre 1982, Vos 1991). An anomaly on the melting curve was detected around 290K, interpreted as a triple point associated to the possible stability of a bcc phase along melting (Levesque 1983, Loubeyre 1986). Direct structural determination by x ray diffraction could only become feasible with the use of high flux synchrotron beam (Mao 1988a). The structural properties, equation of state and phase diagram of He, from low temperature to 400 K and up to 60 GPa, have recently been pinned down (Loubeyre 1993a). The equation of state in the fluid phase has been derived from Brillouin scattering measurements of the sound velocity (LeToullec 1989). The structural properties are a sensitive test of the models of interaction. Shock-wave measurements have aimed to determine a spherically symmetric effective interatomic potential with which statistical mechanics calculations of dense He would be easy and accurate. There exists a significant discrepancy between the best ab-initio or experimental pair potentials and the effective potential derived from shock-wave data (Ross 1989). The latter is softer indicating the existence of many-body interactions. Two theories have been proposed to calculate these many-body interactions: either from the spherical contraction of the electronic

cloud of the He atom in a dense environment (Lesar 1989) or from an effective three-body interaction (Loubeyre 1987a). Refractive index measurements indeed show the contraction of the electronic cloud of He atoms. However, up to now, none of these two forms of interaction explains satisfactorily the phase diagram of He, in particular why is it so different from the ones of heavier rare gas solids. In dense He, quantum effects should originate from the uncertainty principle; they should be well estimated by the  $\hbar^2$  Wigner-Kirkwood expansion or from path integral simulations (Barrat 1989). This gives macroscopic isotopic differences. Measurements of the isotopic shift on the melting curve (Loubeyre 1992) and on the equation of state (Loubeyre 1993) have been reported. Very surprisingly, experiment is inverse of theory, as it will be discussed in section 4.3.

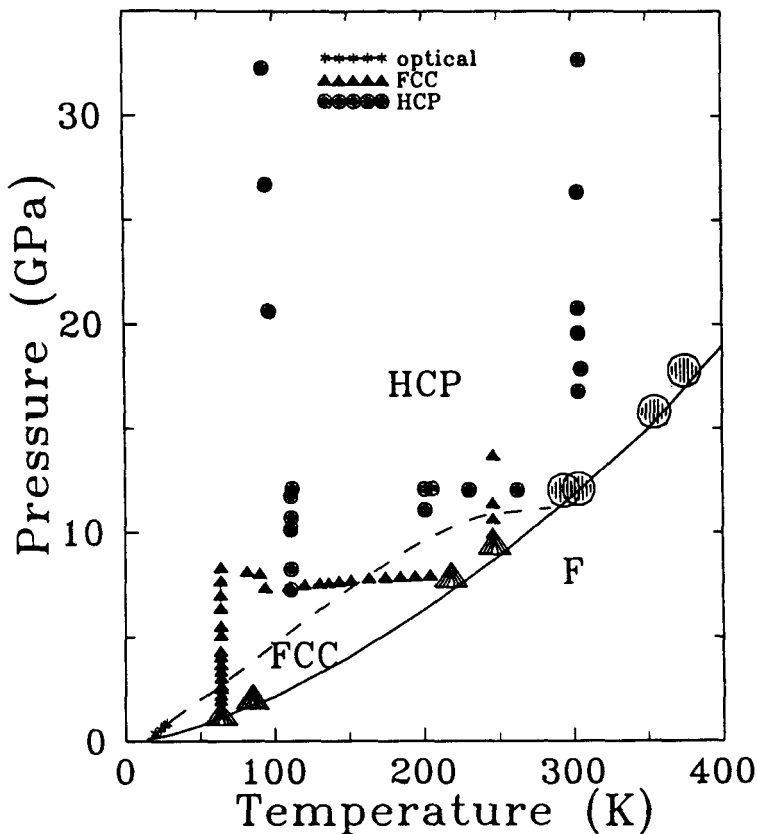


Figure 3: X ray determination of the phase diagram of  $^4\text{He}$ . The large dots and large triangles, respectively, correspond to single crystals of the hcp and fcc structures, for which the orientation matrix was found.

### 11.3.1.2 Mixtures of hydrogen and helium.

$H_2/He$  binary systems were the first mixtures studied in a DAC. Owing to the conceptually simple electronic configuration of the two components, they were considered the most amenable to a theoretical description. Also, its components have been largely investigated under pressure and this should facilitate the analysis of the data. These DAC measurements have been recently used to test various dense mixture theories (Ree 1989, Vos 1991).

The studies of mixtures are generally harder than the ones of pure systems: Great care has to be paid in the control of the concentration loaded in the sample chamber (a mixture of known concentration is loaded with the high pressure vessel technique); Many loadings have to be done to investigate completely the binary phase diagram; Signals get weaker upon dilution.

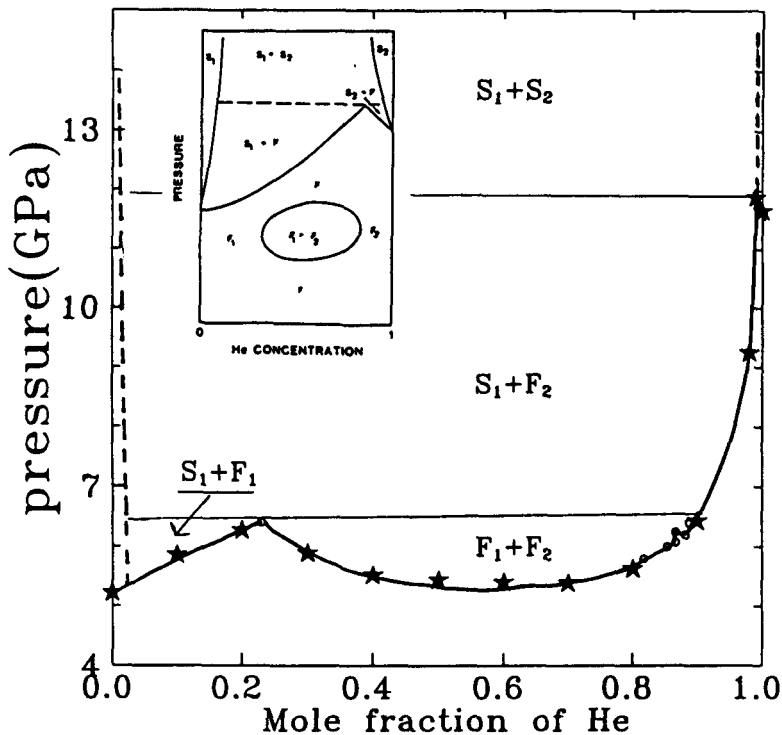


Figure 4: The  $H_2/He$  binary phase diagram at 296 K. A cusp on the  $F_1+F_2$  boundary line has been measured around 90 mol% He. This could indicate a high pressure evolution towards a separation of phases as indicated in the inset.

The binary phase diagram of  $H_2/He$  has been measured from 175 K to 360 K up to 15 GPa (van den Bergh 1987, Loubeyre 1987b 1991). The measurements essentially follow the evolution trend extrapolated from low pressure data (Streett 1973): The binary phase diagram is of eutectic

type with a large fluid-fluid separation phase, between the two triple point at 23 mol% He and 99 mol% He, the pressure domain of which is increasing with temperature. The vibronic properties of the  $H_2$  molecule (intra-molecular frequency) were shown to depend strongly on the concentration of the surrounding mixture (Loubeyre 1985). This was calibrated for use as an in-situ concentration gauge. With it, finer details of the binary phase diagram were observed. In particular, a cusp on the boundary line of the fluid-fluid separation domain, around 90 mol% He, could indicate a different high temperature evolution of the fluid separation of phases, namely the existence of a close fluid-fluid domain at high pressures such as it is represented in the inset of figure 4.

The sound velocity in a mixture of nearly equal concentration was measured by Brillouin scattering (Loubeyre 1993c). Increasing deviation from ideality with pressure is observed. No theory can reproduce, with the same binary potential, the binary phase diagram and the sound velocity of  $H_2$ /He mixtures. Finally, the changes of the properties of the  $H_2$  molecule under strong compression in going from pure hydrogen to the rare gas matrices have been measured (Loubeyre 1992b). In particular, the bond length was found to decrease strongly when the  $H_2$  molecule is embedded in a rare gas matrix (Loubeyre 1991b).

### 11.3.1.3 $H_2$ .

The simplicity of the hydrogen molecule and its large quantum effect in the condensed phase has led to a vast literature, describing subtle molecular processes. The physics at low pressure has been reviewed (Silvera 1980, van Kranendonk 1985). With the advent of the DAC, experimental work on hydrogen under pressure had accelerated sharply.

The  $H_2$  molecule remains a free rotor up to very high pressure and consequently, the ortho-para concentration has a determining role in understanding the phase diagram. At very low temperature, para-hydrogen ( or ortho-deuterium) is a  $J=0$  molecular solid. With pressure, the anisotropic interaction potential becomes sufficiently large, relative to the splitting of the rotational states, so that there is a strong admixture of higher-lying rotational states into the ground state. The lattice spontaneously orders at  $T=0K$  into a structure which minimizes the anisotropic interaction energy. This transition is called the BSP (Broken Symmetry Phase) transition. It has been observed in deuterium at 28 GPa (Silvera 1981), with a transition pressure increasing with temperature, and in hydrogen at 110 GPa and 8 K (Lorenzana 1989). However, the crystal structure of the BSP phase is unknown.

Single-crystal x ray diffraction with a synchrotron source at room temperature shows that the solid structure of normal hydrogen is hcp up to 45 GPa (Hemley 1990, Finger 1991). This has been also obtained by neutron diffraction on deuterium up to 30 GPa (Besedin 1991). The equations of state determined by either neutron or x ray diffraction are identical and show that deuterium is slightly more compressible than hydrogen at the highest pressures. However, none of these structural determinations could give information on the evolution of the molecular bond length with pressure. A spectroscopic determination was made from an analysis of the roton bands at  $T=6\text{K}$  in para- $\text{H}_2$ : The intramolecular distance presents a minimum around 30 GPa (Loubeyre 1991c).

Brillouin scattering measurements give the sound velocities from which the elastic constants, the bulk modulus and the equation of state can be calculated. Measurements in fluid hydrogen at room temperature have produced the equation of state up to solidification (Shimizu 1981). Measurements on a single crystal up to 24 GPa have shown that solid hydrogen is elastically anisotrope (Zha 1993). The equation of state derived from these measurements is in good agreement with the x ray determination.

The melting curves of  $\text{H}_2$  and  $\text{D}_2$  have been measured up to 373 K and 8 GPa (Diatschenko 1985).

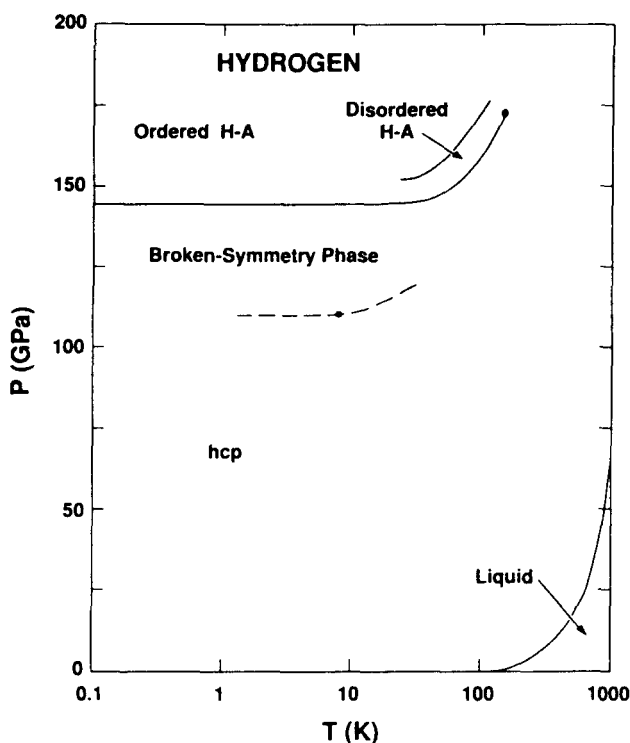


Figure 5: The phase diagram of molecular  $\text{H}_2$  at high pressures.

The very high pressure phase diagram was explored by optical methods, essentially Raman and infra-red measurements of the fundamental excitations of the system, vibrons, rotons, phonons, (Hemley 1991a, Silvera 1991a). The vibron frequency, corresponding to the intramolecular vibration of the  $H_2$  molecule, changes with pressure due to essentially three contributions: The static shift, which is a measure of the crystal compression on the molecule; The vibrational coupling, which results from the resonance transfer of vibrational energy between two neighbour  $H_2$  molecules; The variation of the electronic density going from the intramolecular region to the intermolecular one. The  $H_2$  vibron frequency shows a large discontinuity at 145 GPa and 77K that reveals a first order phase transition to a new molecular phase, named H-A. The same phonon, vibron and roton modes were observed in the hcp solid and in the H-A phase. Also, the frequency of the lattice phonon was observed continuous through the transition. So, it is reasonable to assume that the structure of the molecular centers should be hcp in the H-A phase. The existence of the critical point on the H-A phase line ( 150 K, 165 GPa) implies that there cannot be a change of symmetry at the transition: The molecules should have cylindrically symmetric distribution around the c axis. Orientational transition at the H-A phase transition has been also reported. It has been suspected on a number of grounds that the H-A phase is the metallic molecular phase of hydrogen. Refractive index, absorbance and reflectance measurements have tried to characterize the changes of the electronic properties at the H-A transition, aiming to show the closure of the band gap at 150 GPa. However, at this time, some uncertainty has developed for the support of the conduction state of the H-A phase, as it will be discussed more lengthily in the next section.

The infra-red measurements of the vibron mode have been measured up to 180 GPa by synchrotron infra-red spectroscopy (Hanfland 1992). The difference between the infra-red and the Raman mode indicates a dramatic increase in intermolecular coupling with pressure. Similar results have been obtained by isotopic dilution (Loubeyre 1992).

Clearly, the phase diagram of hydrogen at very high pressure is much more complex than previously imagined. This is certainly a sensitive reference system for testing many-body quantum calculations. This is stimulating high precision theoretical works and the close interaction between theory and experiment should lead to a good description of molecular hydrogen approaching its plasma phase transition.

The above review of the literature is summarized in the table below.

**Table II. Essential measurements on systems of  $H_2$  and He at high pressures.**

SYSTEM	RESULTS.	MAXIMUM PT	REFERENCES
<u>He</u>	Phase diagram, EOS. Melting curve. Isotope effects in dense He. Sound velocity. Refractive index. Hugoniot.	60GPa, 40K-400K 24GPa, 480K 10GPa, 280K 12GPa, 300K 16GPa, 300K 56GPa, 21000K	Loubeyre 1983, Mao 1989 Vos 1990, Loubeyre 1982 Loubeyre 1992 Polian 1986 LeToullec 1989 Nellis 1984
$H_2$	Structure, EOS. Melting. Sound velocity. Bond length. Raman: vibron, phonon, roton. Infra-red: vibron, phonon. Isotopic dilution. Absorbance Reflectance. Refractive index. Hugoniot. Conductivity in shocked $H_2$ .	45GPa, 300K 8GPa, 380K 23GPa, 300K 40GPa, 6K 230GPa, 10K-300K 180GPa, 300K 120GPa, 80K 230GPa, 77K-300K 177GPa, 300K 220GPa, 300K 76GPa, 7000K 120GPa, 3000K	Hemley 1989, Beesdin 1991 Diatschenko 1985 Shimizu 1981, Zha 1993 Loubeyre 1991 Hemley 1991, Silvera 1991 Hanfland 1992 Loubeyre 1991,1993 Eggert 1991, Hanfland 1991 Mao 1990, Eggert 1991 Hemley 1991, Garcia 1992 Nellis 1983 Nellis 1992, Weir 1993
$H_2/He$	Binary phase diagram. Vibron. Sound velocity. Isolation in matrices.	10GPa, 373K 15GPa, 300K 5GPa, 300K 40GPa, 77K	Van Bergh 1987, Loubeyre 1991 Loubeyre 1991 Loubeyre 1993 Loubeyre 1992

### 11.3.2 An important problem: The search for metal hydrogen.

#### 11.3.2.1 Compression of solid $H_2$ .

The formation of metal hydrogen by application of pressure and the characterization of its physical properties is considered a major problem in condensed matter physics (Ginzburg 1983). This should result in the simplest possible metal, with each lattice point in the crystal occupied by a bare proton immersed in a sea of electrons. Theoretical predictions suggest that it will behave as a quantum metal, with properties considerably different from those of simple metals (Ashcroft 1991). The formation of metal hydrogen is of quantum nature (based on the Pauli exclusion principle) as first predicted by Wigner and Huntington (1935). In the original treatment, a first order phase transition takes place from the insulating molecular phase to the monatomic metal. More recently, an other mechanism of metallization has been proposed where an intermediate molecular metal phase will exist (Friedli 1977). In this phase, the solid retains its distinct molecular components with the metallic character achieved by overlap of the valence and the conduction

bands. The knowledge of the sequence of the metallization of hydrogen, the order of the phase transition and the associated latent heat are essential information for describing the interior of giant planets and brown dwarfs.

There are three likely experimental approaches to metallic hydrogen: Static isothermal compression; Isentropic compression; Shock compression. Shock compression leads to temperature that are too high for reaching the required density. Isentropic compression, in a magnetic flux compression device, has been performed and experimentalists have claimed to have produced metallic hydrogen. Unfortunately, only the most primitive diagnostic measurements have been made and the claims remain unconvincing. It recently became clear that the issue of the metallic transition will be settled by DAC technology.

At the low temperature onset of the H-A transition, the discontinuity of the vibron frequency was approximately  $100 \text{ cm}^{-1}$ , much larger than what would be expected from an orientational transition (Hemley 1988, Lorenzana 1989). This discontinuity was not related to a structural phase transition and so could originate from a change in electronic properties. It was suggested that the H-A phase was the molecular metallic phase of hydrogen (Mao 1989, Eggert 1990). So, the decrease of the vibron frequency would correspond to the transfer of electrons from molecular bond states to crystalline band states. Since the inter-proton electronic charge density in hydrogen is responsible for the binding of forces, if this charge density were reduced, it would result in a weaker bond and a lower vibron frequency. The most rigorous mean of establishing this insulator-metal transition is to measure the dc electrical conductivity and to show that it remains finite in the limit that  $T \rightarrow 0\text{K}$ . This is difficult to do in a DAC at megabar pressures. Two experimental groups have opted to study the H-A transition by optical means: dielectric, reflectance and absorbance measurements. These various experiments have been recently reviewed with critical consideration, independently by the leaders of these two groups (Mao 1992, Silvera 1991b). They agree that the experimental situation is unclear and that there is no direct proof of metallization. This is discussed below.

#### *Dielectric measurements.*

The refractive index and its dispersion should reflect changes in the electronic density. These measurements have been performed on hydrogen at visible frequencies up to 170 GPa (Hemley 1991). No evidence of dielectric catastrophe (divergence of the static electric polarizability), which should be associated with free electrons, nor even a measurable discontinuity at the H-A phase transition was observed.

This suggests that if the H-A phase transition is a metal-insulator phase transition, it should be due to the closure of an indirect band gap giving a very small free carrier density. In fact, extracting information on the electronic properties from such measurements is not straightforward. Comparison with full electronic density calculation of the dielectric response was proven useful to interpret similar measurements up to 220 GPa (Garcia 1992).

*Absorption and reflexion measurements.*

In the metallic state, the optical reflectance and absorption could be reasonably described by a Drude free electron model. The Drude model is a three parameter model (plasma frequency, electron relaxation time and the difference in the real part of the dielectric constant at the diamond sample interface). The plasma frequency is proportional to the square root of the charge carrier density. Entire confidence in the applicability of the Drude model must be provided by the demonstration of the consistency of the absorption and reflection data.

Reflectance measurements have been performed (Mao 1990) on solid H<sub>2</sub> to 177 GPa from 0.5 eV to 3 eV. At the highest pressures, they observed a rising reflectivity in their low frequency spectral limit. This was interpreted as a free carrier reflection. Analysis of volume dependence of the plasma frequency obtained from Drude-model fits to the spectra indicates that the pressure of the insulator-metal transition is 149 GPa. Subsequently, the interpretation of these experimental data was questioned (Eggert 1991), by performing absorption and reflection measurements a much higher pressure, 230 GPa, from 0.7 eV to 3 eV. Extrapolating the fit of the plasma frequency of Mao, a strong absorption and reflection should be present in contrast to what was observed. Finally, absorption data were reported (Hanfland 1991) to be consistent with the reflection measurements only under the assumption that at very high pressure the refractive index of diamond gets greater than the one of hydrogen, which seems quite unphysical.

The discrepancy between the measurements of these two groups could arise from various reasons: First, the samples of the two groups are different and anisotropy and crystalline order can significantly shift the optical spectrum; Second, in Mao's experiments, the sample was loaded with ruby powder that at very high pressure could chemically react with hydrogen (Ruoff 1991). Free Al would then dilute in the sample and change the electronic properties. Still, direct experiments seem to infirm these hypothesis (Mao 1991). Third, the simple Drude model used to analyse the data is inappropriate. In summary, these absorbance-reflectance data are confusing and this essentially corroborates the dielectric measurements. No dramatic changes of the electronic properties

are observed above the H-A transition. If H-A were a metallic phase, the number of free electrons should be very small.

*Darkening of the sample.*

In an experiment to 250 GPa at 77K, the hydrogen being in the interstices of a compact ruby powder, darkening of the hydrogen was observed (Mao 1989). However, darkening itself is not a proof of metallization since it could be due to a narrowing of the band gap below the visible wavelengths. Furthermore, the topology of the sample was not ideal for such a report since darkening might be due to the presence of Al liberated by the reaction of hydrogen on ruby.

*Agreement with calculations.*

Following the discovery of the H-A transition, various ab-initio electronic calculations have tried to confirm the interpretation of the closure of an indirect band gap. The structure was assumed to be hcp. However, the orientational distribution of the molecules has a profound effect on the electronic properties. In LDA calculations (Garcia 1990), the hcp structure with spherical charge distribution for the hydrogen molecules which simulates orientational disorder, has a gap closure around 400 GPa whereas, for the hcp structure with the molecules aligned along the c axis, the gap closure is around 180 GPa. Using a quasi-particle calculation, known to give accurate gap results (Chacham 1991), it was found, for the order and disorder hcp structures, band gap closure at respectively 150 GPa and 300 GPa. However, it was later shown that the order hcp structure is not the stabler one; a structure with a molecular orientation with the c axis is stabler but has a wider band gap (Kaxiras 1991). Finally, it was recently shown that the zero-point motion yield important contributions (Surh 1993). So far, no ab-initio theory has been able to identify the observed H-A transition.

Other interpretations of the H-A phase transition could be even more interesting than what we are looking for. There are two conjectured mechanisms by which electrons might be liberated from molecular bonds and yet still not available for molecular conduction: excitonic pairing and dynamic localization. However, no proof for such unusual state of matter has been reported (Ashcroft 1991).

By increasing further the pressure, there is almost no doubt that hydrogen will form the long-sought atomic metal. All recent calculations converge for a transition pressure around 300 GPa (Ceperley 1987). Unfortunately, no progress in the maximum pressure achieved on solid H<sub>2</sub> has been reported since 1989: It could be that the chemical attack of the diamond anvils by hydrogen limits compression further. A new

Raman feature appearing at  $240\text{ cm}^{-1}$ , with an onset pressure from 150 GPa to 200 GPa only when hydrogen or deuterium is in contact with the diamond tip, sustains this assumption (Hemley 1992). Approaches for reducing the pressure of the atomic metal transition are needed to circumvent this problem. This has been achieved recently by the discovery of a new molecular compound,  $\text{Ar}(\text{H}_2)_2$ .

#### 11.3.2.2 *A new path: the compression of $\text{Ar}(\text{H}_2)_2$ compound.*

It has been recently discovered that under pressure simple molecular systems can form ordered alloys. The first two examples found were  $\text{Ne}(\text{He})_2$  (Loubeyre 1993b) and  $\text{He}(\text{N}_2)_{11}$  (Vos 1992). Subsequently, the  $\text{Ar}(\text{H}_2)_2$  compound was solidified at 4.3 GPa. Synchrotron single crystal x ray diffraction showed that its structure is hexagonal with 4 Ar atoms and 8  $\text{H}_2$  molecules in the unit cell. This structure is well-known as a Laves phase. Its stability can be understood from considerations of the maximization of the packing fraction. Interestingly, the  $\text{H}_2$  molecules are arranged at the corner of tetrahedra which are joined point to point and alternately base to base throughout space, forming long chains. This quasi-1 dimensional alignment offers the possibility to reduce the insulator-metal transition pressure of the hexagonal sublattice of  $\text{H}_2$  molecules. Raman measurements of the vibron and roton modes and absorbance measurements (from 1.4 eV to 3.0 eV) were performed up to 200 GPa twice on  $\text{Ar}(\text{H}_2)_2$  and once on  $\text{Ar}(\text{D}_2)_2$  compounds (Loubeyre 1993c). A first order phase transition was observed at 175 GPa. It is associated with the disappearance of the vibron mode (signature of the molecular entity), a visual increase in absorbance of the sample, a possible Drude edge in the absorption spectra (indicative of free carriers) and in good agreement with theoretical predictions of metallization in the m-hcp structure of pure solid  $\text{H}_2$  that is similar to the sublattice of the  $\text{H}_2$  molecules in this compound. Although none of the facts alone is sufficient at present to prove definitively that metallization has occurred, their conjunction argues strongly for the observation of the metallization/dissociation by pressure of this system of hydrogen molecules. The Ar atoms should remain neutral. The physics involved in the metallization of this hexagonal sub-lattice of  $\text{H}_2$  is consequently equivalent to what could be found in metallizing solid  $\text{H}_2$ . So it is now very interesting to try to fully characterize the properties of this new metal of hydrogen.

## **Ar(H<sub>2</sub>)<sub>2</sub> compound**

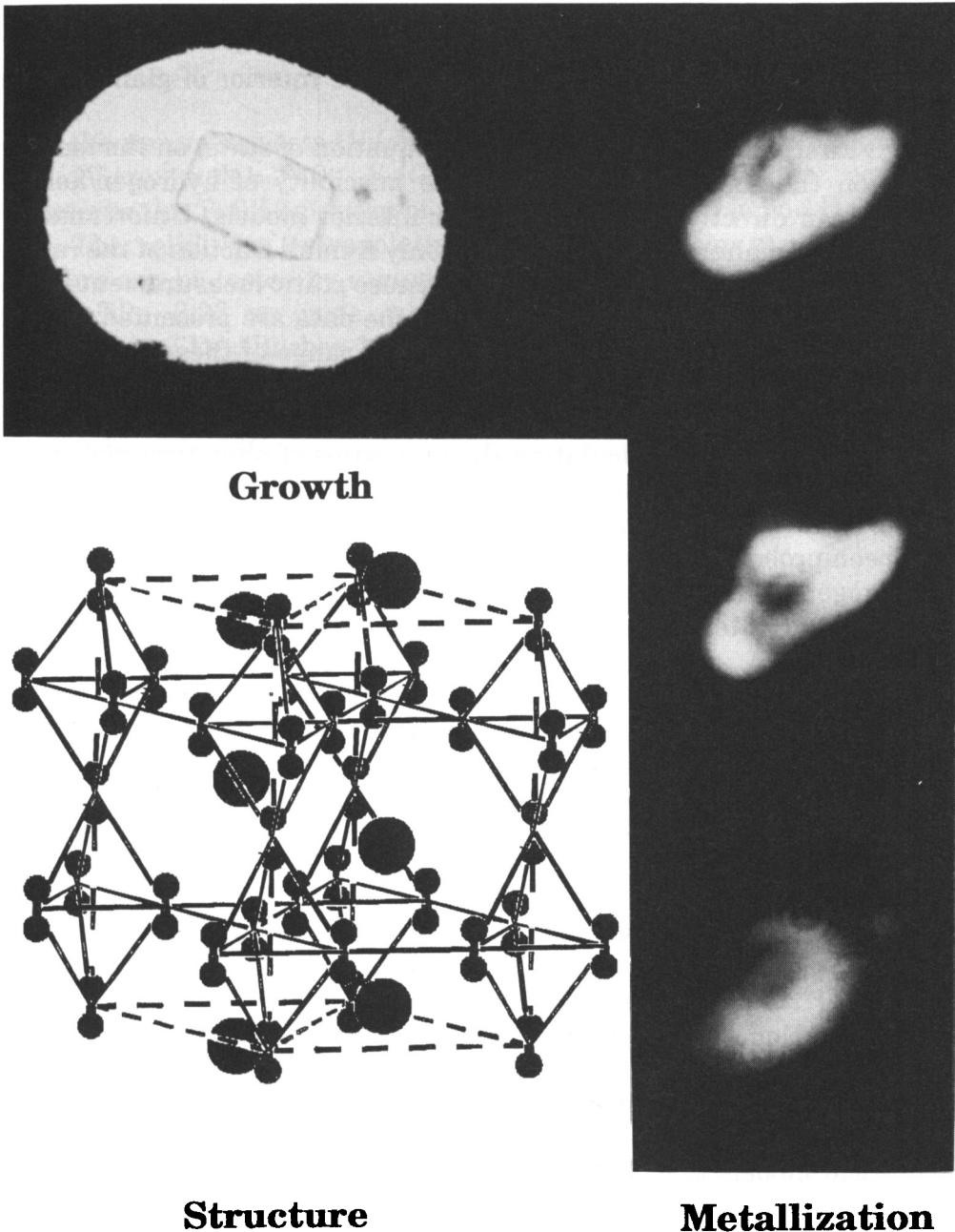


Figure 6: Three observations on the Ar(H<sub>2</sub>)<sub>2</sub> compound. Growth: faceted hexagonal single-crystal in equilibrium with a fluid of equal concentration. Structure: hexagonal structure with 8 H<sub>2</sub> molecules and 4 Ar atoms in the unit cell. Metallization: First order phase transition at 175 GPa (sample chamber 10 μm diameter with a small ruby) associated to a disappearance of the vibron and a visual increase in absorbance.

## 11.4 Usefulness of high pressure measurements for Astrophysics.

Three levels of usefulness can be distinguished in the use of high pressure measurements for understanding the interior of giant planets and brown dwarfs.

-First, experimental data on the equation of state, on the melting curve, on the sound velocity or on the miscibility of hydrogen/helium systems can directly serve as input for interior models. Unfortunately, the PT domain already explored covers only a small fraction of the radius of these astrophysical objects, mainly because static measurements were done up to now below 400 K. However, if the data are presented in form of fits that have a physical meaning, the PT range of these data can be significantly extended.

-Second, the experimental data can be used to test the assumptions made for calculating the properties of planetary matter. In such calculations, the significant parameter is density rather than pressure or temperature. Properties of hydrogen and helium systems have been probed to densities at the limit of the plasma phase transition in hydrogen. The accuracy of the description of the whole molecular domain of the interior of giant planets and brown dwarfs could now be assessed.

-Third, the study of matter at the frontier of investigation can reveal subtle behaviours of matter, generally unsuspected.

Below, we illustrate this classification with a selection of some of the experimental data that were reviewed in the preceding section.

### 11.4.1. *Data for codes.*

#### 11.4.1.1 *Equation of state.*

X ray diffraction measurements give a direct and accurate determination of the equation of state in the solid phase. Shock-wave experiments provide an indirect determination by the fit of an effective symmetric effective intermolecular interaction which can be used with accurate theoretical models to calculate the equation of state. In figure 7, these two determinations are compared for H<sub>2</sub> and for He solids. An increasing difference with pressure between them is observed. This is a consequence of the growing importance of many-body interactions. Their pair average, which is incorporated in the effective pair interaction, depends on the structural state of the system: the average in the high temperature shock-fluid differs from the one in the solid state at the same density. The x ray data, combined with previous low pressure data, were shown

to be well-represented by the two-parameter Vinet equation:

$$P=3K_0\left(\frac{V}{V_0}\right)^{-\frac{2}{3}}\left(1-\left(\frac{V}{V_0}\right)^{\frac{1}{3}}\right)\exp\left(\frac{3}{2}(K_0'-1)\left(1-\left(\frac{V}{V_0}\right)^{\frac{1}{3}}\right)\right)$$

With the parameter sets ( $V_0(\text{cm}^3/\text{mole})=13.72$ ,  $K_0(\text{GPa})=0.225$ ,  $K_0'=7.35$ ) and ( $V_0(\text{cm}^3/\text{mole})=23.0$ ,  $K_0(\text{GPa})=0.172$ ,  $K_0'=7.19$ ), this equation represents the  $T=0\text{K}$  equation of state of respectively He and  $\text{H}_2$  above 1 GPa. The validity of extrapolating the Vinet equation at much higher pressure can be tested by comparing the volume estimated for solid  $\text{H}_2$  at 200 GPa,  $2.23 \text{ cm}^3/\text{mole}$ , with the ones obtained from two ab-initio calculations, LDA (Barbee 1989) and QMC (Ceperley 1987), respectively  $2.0 \text{ cm}^3/\text{mole}$  and  $2.44 \text{ cm}^3/\text{mole}$ . It falls in-between these two theoretical determinations; Still, the uncertainty on the EOS of  $\text{H}_2$  above 150 GPa is quite large,  $\approx 20\%$ .

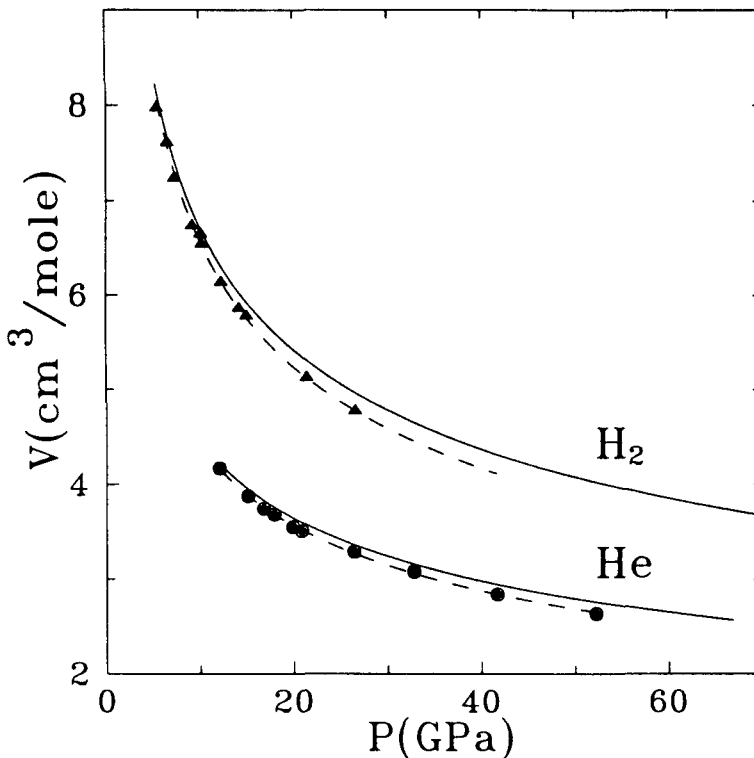


Figure 7: Equations of state of He and  $\text{H}_2$ . The dots and triangles are the x ray data respectively for He and  $\text{H}_2$ . The dashed-lines are the Vinet fits. The solid line is the EOS calculated from the pair interactions derived from shock-wave.

#### 11.4.1.2 Melting curve.

The melting data of  $\text{H}_2$  and He, respectively up to 360 K and 400 K, are

well represented by the Simon law,  $P=AT^c+B$ .

$$\begin{aligned} \text{For He, } P(\text{GPa}) &= 1.607 \cdot 10^{-3} T(\text{K})^{1.565} \\ \text{For H}_2, P(\text{GPa}) &= -0.052 + 3.436 \cdot 10^{-4} T^{1.691} \end{aligned}$$

In figure 8, these Simon equations are compared over an extended temperature range to the melting curves calculated with the interactions adjusted on the shock-wave Hugoniot (Young 1981, Ross 1983). These theoretical melting curves should not be too far from the true experimental curves, with the limitation that the above discussion on the effective effect of many-body interaction still operates here. The extrapolation of the Simon equation is more questionable. The repulsive part of the real interaction in very dense  $\text{H}_2$  and He is getting softer with density, similarly to an  $e^{-\alpha r}$  behaviour. From scaling arguments, it can be shown that the melting curve should become with pressure increasingly steeper than the Simon equation, tending towards a temperature maximum (Loubeyre 1989).

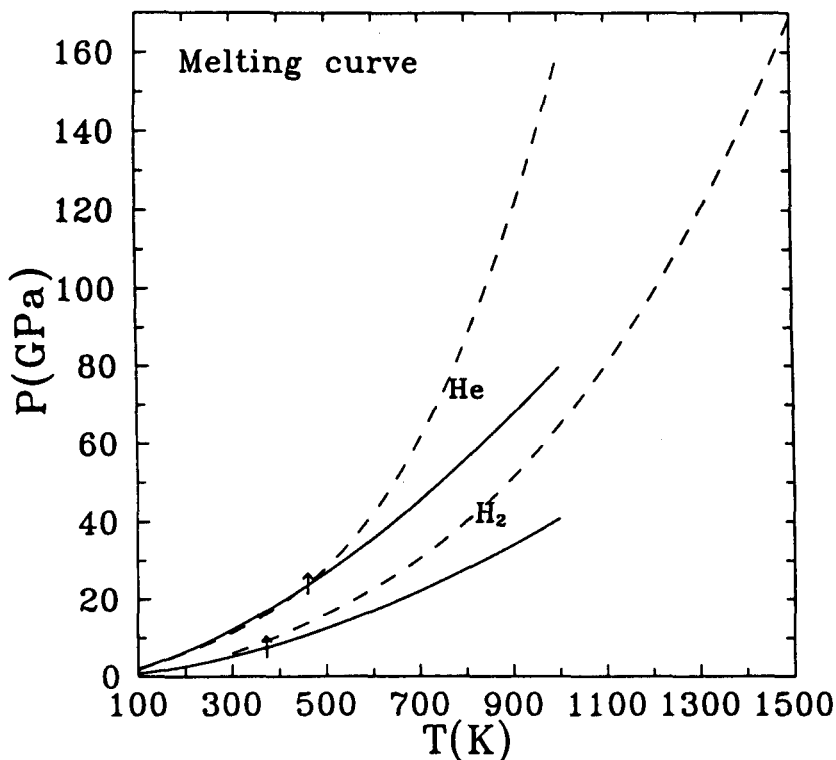


Figure 8: Evolution at very high pressures of the melting curves of  $\text{H}_2$  and He. The solid lines represent the Simon equations. The dashed-lines are the calculation with the pair interactions adjusted on shock-wave. The arrows indicate the maximum temperature of the measurements.

### 11.4.1.3 Sound velocity.

In figure 9, the adiabatic sound velocities in liquid He (Polian 1986) and in liquid H<sub>2</sub> (Shimizu 1981) are plotted versus density at room temperature. A linear relation is observed above 0.13 g/cm<sup>3</sup> in liquid H<sub>2</sub> and above 0.45 g/cm<sup>3</sup> in liquid He. This linearity is well-known in geophysics as the Birch law. From analysis in the dense solid phase, it seems that this relation should also be valid at much higher density (Loubeyre 1990). Still, no theoretical justification has been given. Certainly, this form should be useful to extrapolate experimental data.

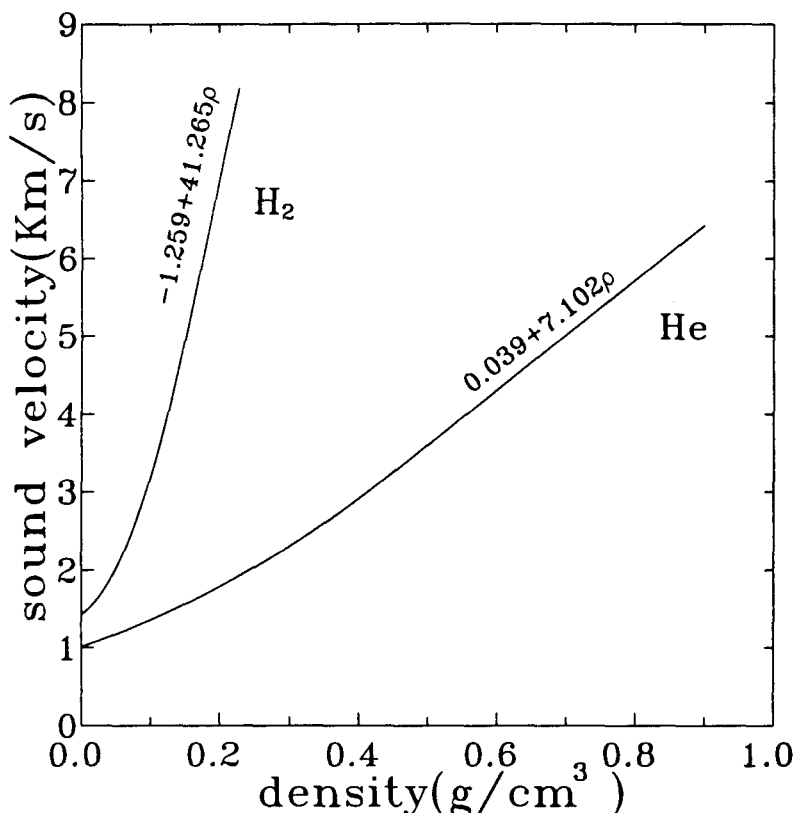


Figure 9. Adiabatic sound velocity versus density at 296 K. A linear relation is observed above 0.13 g/cm<sup>3</sup> in fluid H<sub>2</sub> and above 0.45 g/cm<sup>3</sup> in fluid He.

### 11.4.1.4 Miscibility.

The binary phase diagram of the H<sub>2</sub>/He binary mixtures is of eutectic type with a large fluid-fluid separation of phase, as shown in figure 4. At a given temperature, the pressure interval of the fluid-fluid domain is lower-bounded by the pressure of the critical point and upper-bounded by the pressure of the fluid-fluid-solid triple point, above which solid separation of phase exists. The PT loci of these points, namely the critical line and the triple line, give the essential information on the pressure

evolution of the miscibility of the system. From figure 10, it is likely that the fluid-fluid equilibrium of  $\text{H}_2/\text{He}$  mixture will persist up to very high pressure (van den Bergh 1987). However, a small accident on the fluid-fluid boundary line around 90 mol% He was interpreted as a preliminary sign of the evolution towards a re-entrant fluid domain (Loubeyre 1987), as drawn in the inset of figure 4. It is too early to conclude. High temperature experiments have to be performed beforehand.

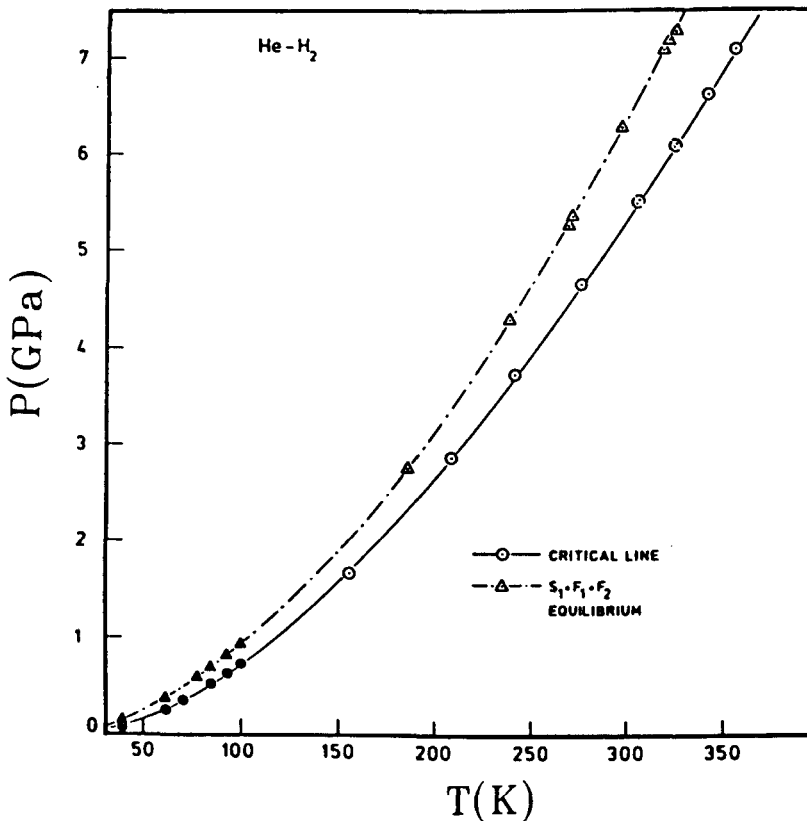


Figure 10: Critical line and three phase line in the  $\text{He}/\text{H}_2$  system (van den Bergh 1987).

#### 11.4.2 Constraints for theoretical description.

The calculation of the physical properties of the  $\text{H}_2/\text{He}$  molecular envelop of low mass star interiors up to the plasma phase transition is difficult. The ab-initio approach, which starts with the coulombic hamiltonian of the system, presents convergence uncertainties when the electrons are localized in molecular entities. As seen above, the difference in the EOS of molecular  $\text{H}_2$  by two state-of-the-art ab initio methods, QMC and LDA, amounts to 20% at 200 GPa. Also, these calculations are mostly limited to  $T=0\text{K}$ . That is why the molecular approach is generally used instead. It is based on the description of the interactions between molecular

entities. With well-known statistical methods, calculations of the physical properties of the system at arbitrary PT conditions can then be made. The interactions are generally assumed of pair potential forms, which are adjusted on high pressure measurements. It will be shown below that many-body interaction and charge transfer between  $H_2$  molecules approaching the plasma phase transition complicate this description. Sometimes, it could thus be better to use extrapolation of high pressure experimental data. The properties of  $H_2/He$  mixtures are harder to calculate and to measure than the ones of the pure systems. So, they are generally estimated from the properties of the two pure components with the law of ideal mixing, i.e. extensive variables are additive. This approximation will be questioned experimentally below.

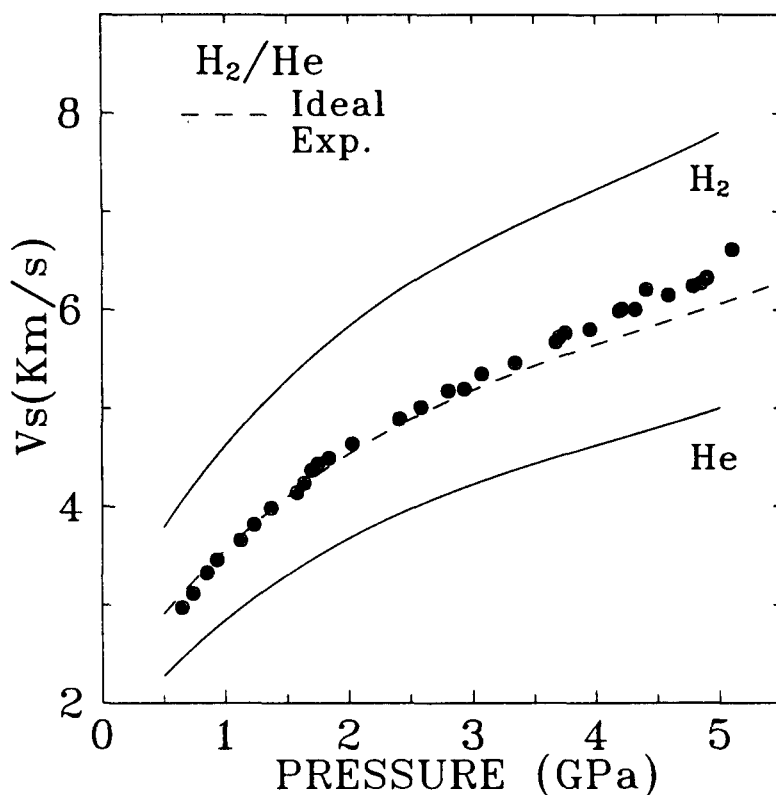


Figure 11: Adiabatic sound velocities in fluid He (solid line), fluid  $H_2$  (solid line) and  $H_2/He$  fluid mixture of 52 mol% in  $H_2$  (the dots are the Brillouin data and the dashed line is the ideal mixture calculation).

#### 11.4.2.1 Ideality.

For an ideal mixture, the extensive variables add. There is no phase separation. Applied to the EOS, it means the additivity of the volumes of the two components,  $v_M(x) = x v_{He} + (1-x) v_{H_2}$ . The volume of mixing quantifies the deviation from this behaviour but it is a difficult quantity

to measure at high pressure. A related property is the sound velocity that can be measured by Brillouin scattering experiment. In figure 11, the sound velocity measured in a fluid  $H_2/He$  mixture of 52 mol%  $H_2$  (Loubeyre 1993d) is compared to the ideal mixing calculation from the measurements in pure  $H_2$  and pure He. A discrepancy appears increasingly with pressure. Even at the moderate density of the experiment, the error already amounts to 6%. The volume is related to the integral of an expression which contains the sound velocity to the square. So, the deviation from ideal mixing could even be greater for the equation of state than for the sound velocity. This casts some doubts about the validity of the use of the law of additive volume for planetary interior models.

#### 11.4.2.2 *Interactions in the molecular phase.*

The pair potential adjusted on high pressure data differs from the truly pair interaction between two isolated molecules. The repulsive part of the former is significantly softer. This experimental potential is an effective potential that includes many-body interactions. Physically, the deformation of the electronic cloud of a molecular entity in a dense environment modifies the interaction energy between two such electronic cloud: This is the many-body contribution. Electrons of  $H_2$  molecules are loosely bound to nuclei and easily change their charge density when other molecules are placed nearby whereas in He, the tightly bound electrons are less subject to change. Many-body contributions should be greater in  $H_2$  than in He.

It has been shown above that the  $T=0K$  solid EOS calculated with effective pair potential fitted on Hugoniot, increasingly differs with pressure from the x ray determination. This shows the limit of this effective pair potential approach: the environment of an interacting molecular pair is different in a dense solid than in a shocked high temperature fluid, even at the same density. So, the effective many-body contribution to the pair potential interaction should be structure dependent. Two models have been proposed to consider this many-body contribution more explicitly. In the first one, a sphericalized contraction of the electronic cloud is calculated by Gordon-Kim-Hartree-Fock method (LeSar 1988). In the second one, a three body interaction is assumed to be the essential term and is added to the pair potential (Loubeyre 1987a). As seen in figure 12, the EOS calculated with these two approaches are in fair agreement with experiment, although none will be entirely satisfactory at higher density. The strong difference, between the calculated EOS with the pure pair potential calculated EOS and the experimental one, quantifies the contribution of the many-body

interaction in dense He. In dense  $H_2$ , this term is more important and the situation is further complicated by the charge transfer interaction.

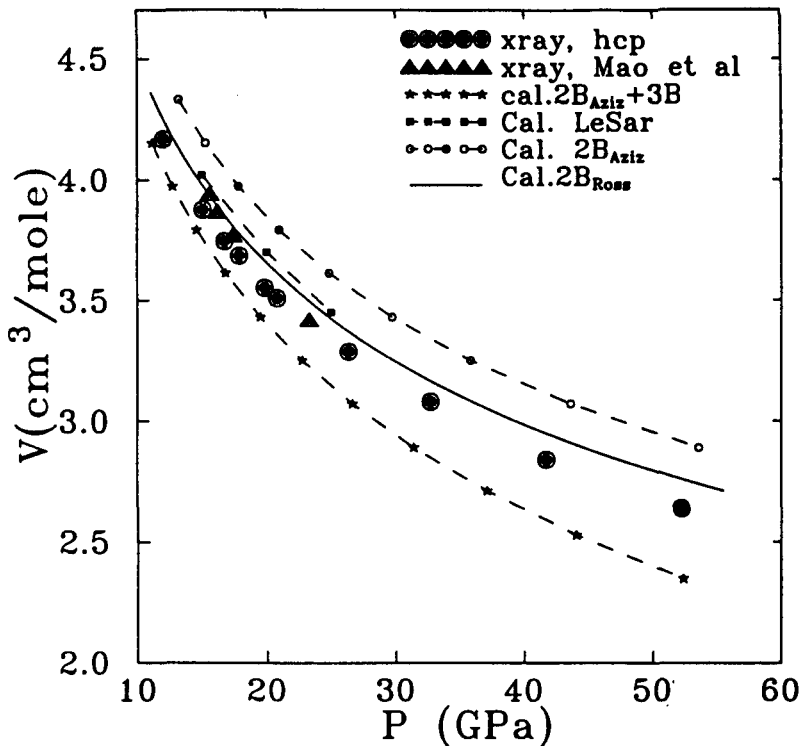


Figure 12: Volume versus pressure data of hcp solid  ${}^4\text{He}$  at 304 K. The dots and squares indicate x ray measurements. Four calculated EOS are compared: self-consistent phonon calculations either with the HFD-B pair potential (dash-dotted line), the Ross-Young potential (full line), the HFD-B pair potential plus three body interaction (dashed-stars line). The dashed-squares line is the LeSar many-body calculation.

When two  $H_2$  molecules are brought close to one another with density, the probability increases that electrons exchange through a mechanism involving electron tunnelling. This leads to an attractive interaction like the beginning of a covalent bonding. An experimental indication of it is presented in figure 13. In hcp solid, there are two vibron modes: one, which corresponds to the coupled in phase motion of the two intramolecular vibrations in the unit cell, is raman active and the other one, which corresponds to the uncoupled motion, is infra-red active. The difference between these two modes is due to the vibrational coupling. The associated vibrational coupling constant is negative and increases with density, as seen in the inset of figure 13. This is unexpected for intermolecular distances corresponding to the strongly repulsive overlap

intermolecular interaction and could be the indication of a charge transfer interaction. It contributes to the extra softening of the pair interaction but no model has been proposed so far to explicitly describe this interaction.

The situation is even more complicated in mixtures because the concentration parameter affects the environment of an interacting molecular pair. The effective pair potential should thus be concentration dependent. No approach based on effective pair potentials can satisfactorily describe the  $H_2/He$  binary mixtures: the  $H_2$ -He potential that is fitted on the binary phase diagram cannot reproduce sound velocity measurements and vice versa. Since re-entrant fluid phases in binary mixtures are generally attributed to the existence of an attractive interaction (like the hydrogen bond in water-alcohol mixtures), the observed cusp on the fluid-fluid boundary line of the  $H_2/He$  binary phase diagram would probably be reproduced by explicitly considering the attractive charge transfer interaction between  $H_2$  molecules.

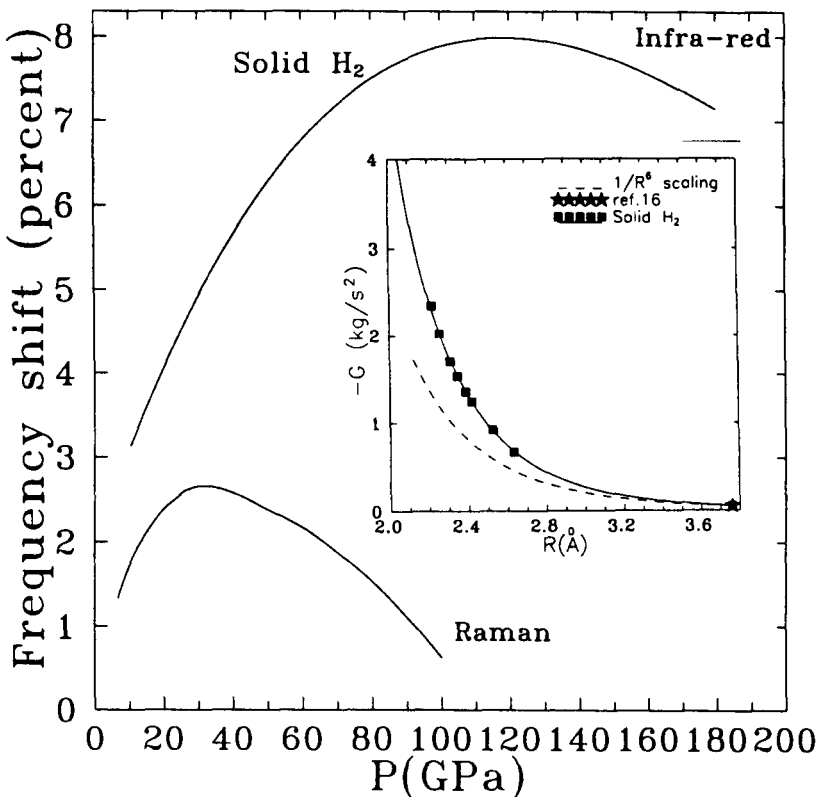


Figure 13: Pressure dependence of the Raman and infra-red vibrons of hcp solid  $H_2$ . Their difference is due to the vibrational coupling. The negative of the vibrational coupling constant is plotted versus the intermolecular distance in the inset.

In summary, deviations from the pure pair potential interaction are important at high density. Their pair average in an effective pair interaction fitted on experimental data only gives a first description: interesting properties can be missed. More works are needed to find out mathematical forms that can satisfactorily represent many-body and charge transfer interactions.

#### 11.4.3 *Unsuspected properties.*

Observing properties that were unsuspected or doing measurements that are in strong disagreement with the best theoretical predictions generally creates new physical approaches. In the experimental investigation of the properties of matter under very high pressure, this is all the more so to happen in the studies of  $H_2$  and He systems due to their electronic simplicity and their quantum nature. Indeed, the measurements of the quantum properties of He at high density have recently offered such a surprise.

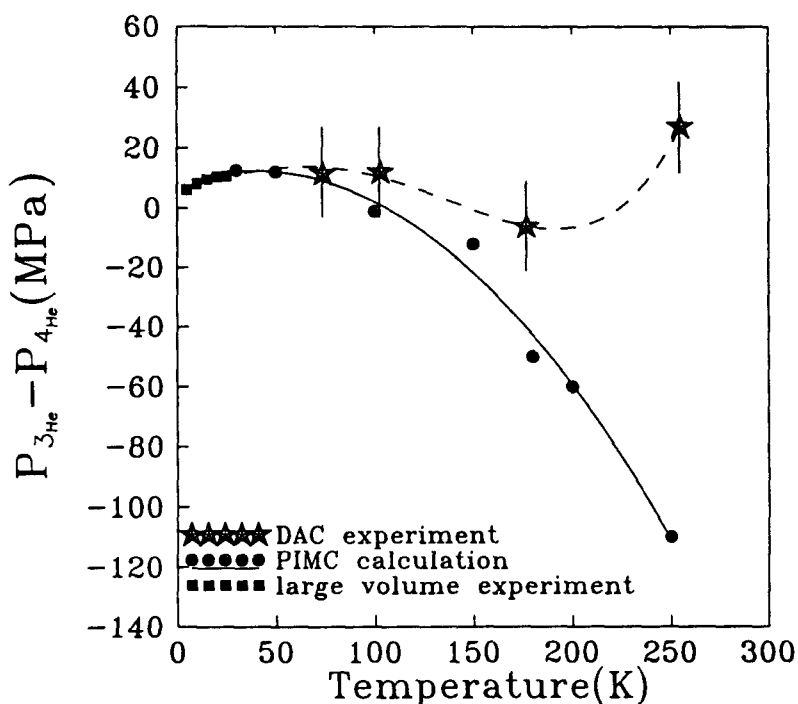


Figure 14: Difference between the melting pressures of  $^3\text{He}$  and  $^4\text{He}$  versus temperature. The stars and the squares are experimental data. The circles are the results of the PIMC simulation.

With increasing density in He, the effect of statistics should become

negligible, even at very low temperature, because of the hindered density fluctuations by the core potential. On the other hand, quantum effects associated with the uncertainty principle should give measurable isotopic differences between macroscopic properties of  $^3\text{He}$  and  $^4\text{He}$ . The isotopic shift in the melting curve of He has been measured from 70 K to 260 K in a DAC (Loubeyre 1992a), extending previous large volume experiments done up to 30 K. In figure 14, these measurements are compared to a path integral Monte Carlo calculation (PIMC) which should be very close to a quasi-exact answer under the following three assumptions (Barrat 1989): the effects of statistics are negligible; the many-body interaction can be included in an effective pair potential and finally the Born-Oppenheimer approximation is valid. A discrepancy occurs with pressure, leading to an opposite isotopic shift above 200 K. When plotted versus the nearest neighbour interatomic distance, the difference between theory and experiment is of a regular exponential form. So, at least one of the three assumptions made prior the PIMC should be violated. The very recent measurement of the isotopic shift on the EOS of He at  $T=300$  K has enabled to specify a bit more this problem. The EOS of  $^3\text{He}$  and  $^4\text{He}$  are observed to cross around 22 GPa,  $^3\text{He}$  being notably more compressible than  $^4\text{He}$  at high pressures. This is unusual and corroborates the observation of the inverse isotopic shift on the melting curve. This seems to favour the interpretation of important effects of statistics at very high density. This unsuspected behaviour could be even more dramatic at high density. Further works are needed to come up with a definite interpretation.

### 11.5 Conclusion.

I have tried to review the status of the experimental investigation of the equation of state for Astrophysics. The subject was limited to the properties of the two major components of the low-mass astrophysical objects,  $\text{H}_2$  and He. It should be noted that the properties of denser elements, such as ices, have been also thoroughly investigated at high density by shock-wave or static DAC experiments. Rapid progress have been made in the past decade and densities characteristic of the molecular envelop of planets can now be achieved in static experiments. Even though these experiments have been performed at low temperatures ( $<400$  K), the above discussion aimed at showing how these measurements are relevant for astrophysics. Due to the electronic simplicity of the He and  $\text{H}_2$  elements, two other levels of usefulness have been distinguished that broadens the sole exploitation of the raw data, namely: experimental references to test theoretical descriptions of dense

matter and implications of unsuspected behaviour.

Now, the experimental efforts will try to extend the PT range of the static exploration. Generation of static pressures over 300 GPa on H<sub>2</sub> should enable the observation and characterization of atomic metal hydrogen (as discussed above, the chemical reactivity of hydrogen on the diamond tip will have to be suppressed). Also, an important goal is to couple high temperatures with high static pressures. This is required to extend at higher density most of the measurements presented here: melting curves, H<sub>2</sub>/He binary phase diagram, sound velocity in the fluid phase... Recent technological developments give confidence that temperatures up to 1500 K will be coupled to static high pressures in the near future. Generation of higher temperatures, that will requires the laser heating technique (already use for studying geophysical compounds), is the challenge for the next decade. By achieving it, the molecular layers of the Jovian planets will become transparent. Observations of the Jovian planets will thus give direct information on the ionised layer, or equivalently on the physical properties of a strongly coupled plasma. One can say that the Jovian planets are the high pressure laboratories of tomorrow. Its exploitation will certainly be of considerable interest for the condensed matter community.

#### Acknowledgements.

I thank R. LeToullec and J.P. Pinceaux for helpful discussions and encouragements. This work was supported by the Commissariat à l'Energie Atomique under grant N°: DAM/CEL-2561/3272, NATO under grant N°: CRG-890084 and CNRS.

#### References

- Ashcroft N.W., in *Frontiers of High Pressure Research*, Edit. Hochheimer and Eters R.D., p.115 ( Plenum 1991)
- Barbee T.W.III, Garcia A., Cohen M.L. and Martins J.L., *Phys. Rev. Lett.* 62, 1150, (1989)
- Barrat J.L., Loubeyre P. and M.L. Klein, *J. Chem. Phys.* 90, 5644, (1989)
- Bessedin S.P., Makarenko I., Stishov S.M., Glazkov V.P., Goncharenko I., Irodova A., Somenkov V. and Shil'stein S., in *Molecular Systems Under High Pressure*, Edit. Pucci R. and Piccitto G. (North-Holland, 1991)
- Besson J.M. and Pinceaux J.P., *Science* 206, 1073, (1979)
- Ceperley D.M. and Alder B.J., *Phys. Rev. B* 36, 2092, (1987)
- Chacham H. and Louie S.G., *Phys. Rev. Lett.* 66, 64, (1991)
- Diatschenko V., Chu C.W., Liebenberg D.H., Young D.A., Ross M. and Mills R.L., *Phys. Rev. B* 32, 381, (1985)
- Eggert J.H., Goettel K.A. and Silvera I.F., *Europhys. Lett.* 11, 775, (1990)

- Eggert J.H., Moshary F., Evans W.J., Lorenzana H.E., Goettel K.E. and Silvera I.F., *Phys. Rev. Lett.* 66, 193, (1991)
- Finger L.W., Mao H.K., Hemley R.J. and Hu J., *Bull. Am. Phys. Soc.* 36, 529, (1991)
- Friedli C. and Ashcroft N.W., *Phys. Rev. B* 16, 662, (1977)
- Garcia A., Barbee T.W. III, Cohen M.L. and Silvera I.F., *Europhys. Lett.* 13, 355, (1990)
- Garcia A., Cohen M.L., Eggert J.H., Moshary F., Evans W.J., Goettel K.A. and Silvera I.F., *Phys. Rev. B* 45, 9709, (1992)
- Ginzburg V.L., *Waynflete lectures on Physics* (Pergamon 1983)
- Hawke P.S., Burgess T.J., Duerre D.E., Huebel J.G., Keeler R.N., Klapper H. and Wallace W.C., *Phys. Rev. Lett.* 41, 994, (1978)
- Hanfland M., Hemley R.J. and Mao H.K., *Phys. Rev. B* 43, 8767, (1991)
- Hanfland M., Hemley R., H.K. Mao and Williams G.P., *Phys. Rev. Lett.* 69, 1129, (1992)
- Hemley R.J. and Mao H.K., *Phys. Rev. Lett.* 61, 857, (1988)
- Hemley R., Mao H.K., Finger L.W., Jephcoat A.P., Hazen R.M. and Zha C.S., *Phys. Rev. B* 42, 6458, (1990)
- Hemley R.J., Mao H.K. and Hanfland M., in *Molecular Systems under High Pressure*, Edit. Pucci R. and Piccitto G., p. 223, (North-Holland 1991a)
- Hemley R.J., Hanfland M. and Mao H.K., *Nature* 350, 488, (1991b)
- Hemley R.J. and Mao H.K., *Phys. Lett. A* 163, 429, (1992)
- Jayaraman A., *Rev. Mod. Phys.* 55, 65, (1983); *Rev. Sci. Instr.* 57, 1013, (1986)
- Jeanloz R., *Annu. Rev. Earth Planet. Sci.* 18, 357, (1990)
- Kaxiras E., Broughton J. and Hemley R.J., *Phys. Rev. Lett.* 67, 1138, (1991)
- Klepeis J.E., Schafer K.J., Barbee T.W. III and Ross M., *Science* 254, 986, (1991)
- LeSar R., *Phys. Rev. Lett.* 61, 2121, (1988)
- LeToullec R., Pinceaux J.P., Loubeyre P., *High Press. Res.* 1, 77, (1988)
- LeToullec R., Loubeyre P. and Pinceaux J.P., *Phys. Rev. B* 40, 2368, (1989)
- Levesque D., Weis J.J. and Klein M.L., *Phys. Rev. Lett.* 51, 670, (1983)
- Lorenzana H.E., Silvera I.F. and Goettel K.A., *Phys. Rev. Lett.* 63, 2080 (1989)
- Lorenzana H.E., Silvera I.F. and Goettel K.A., *Phys. Rev. Lett.* 64, 1939 (1990)
- Loubeyre P., Besson J.M., Pinceaux J.P. and Hansen J.P., *Phys. Rev. Lett.* 49, 1172, (1982)
- Loubeyre P., LeToullec R. and Pinceaux J.P., *Phys. Rev. B* 32, 7611, (1985)
- Loubeyre P., *Physica* 139&140, 224, (1986)
- Loubeyre P., *Phys. Rev. Lett.* 58, 1857, (1987a)
- Loubeyre P., LeToullec R. and Pinceaux J.P., *Phys. Rev. B* 36, 3723 (1987b)
- Loubeyre P., in *Simple Molecular Systems at Very High Density*, Edit. Polian A., Loubeyre P. and Boccara N., p. 181 (Plenum 1989)
- Loubeyre P. and LeToullec R., *High Press. Res.* 3, 263, (1990)
- Loubeyre P., LeToullec R. and Pinceaux J.P., *J. Phys. Condens. Matter* 3, 3183, (1991a)
- Loubeyre P., LeToullec R. and Pinceaux J.P., *Phys. Rev. Lett.* 67, 3271, (1991b)
- Loubeyre P., Jean-Louis M. and Silvera I.F., *Phys. Rev. B* 43, 10191, (1991c)
- Loubeyre P., in *Simple Molecular Systems under High Pressure*, Edit. Pucci R. and Piccitto G. (North-Holland 1991d)
- Loubeyre P., LeToullec R. and Pinceaux J.P., *Phys. Rev. Lett.* 69, 1216, (1992a)
- Loubeyre P., LeToullec R. and Pinceaux J.P., *Phys. Rev. B* 45, 12844, (1992b)
- Loubeyre P., LeToullec R., Pinceaux J.P., Mao H.K., Hu J. and Hemley R., *Phys. Rev. Lett.* 71, 2272, (1993a)
- Loubeyre P., Jean-Louis M., LeToullec R. and Charon-Gérard L., *Phys. Rev. Lett.* 70, 178 (1993b)
- Loubeyre P., LeToullec R. and Pinceaux J.P., to be published in *Phys. Rev. Lett.* (1993c)
- Loubeyre P. and Polian A., private communication (1993d)
- Manghani M.H. and Syono Y. edit., *High Pressure research in Mineral Physics* (KTK

- Scientific, Tokyo 1987)
- Mao H.K. and Bell P.M., *Science* 203, 1004, (1979)
- Mao H.K., Xu J. and Bell P.M., *J. Geophys. Res.* 91 B5, 4673, (1986)
- Mao H.K. Jephcoat A.P., Hemley R.J., Finger L.W., Zha C.S., Hazen R.M. and Cox D.E., *Science* 239, 1131, (1988a)
- Mao H.K., Hemley R.J., Jephcoat A.P., Finger L.W., Zha C.S. and Bassett W.A., *Phys. Rev. Lett.* 60, 2649, (1988b)
- Mao H.K. and Hemley R.J., *Science* 244, 1462, (1989)
- Mao H.K., Hemley R.J. and Hanfland M., *Phys. Rev. Lett.* 65, 484, (1990)
- Mao H.K., Hemley R.J. and Hanfland M., *Phys. Rev. B* 45, 8108, (1992a)
- Mao H.K. and Hemley R.J., *American Scientist* 80, 234 (1992b)
- Nellis W.J., Ross M., Mitchell A.C., van Thiel M., Young D.A., Ree F.H. and Trainor R.J., *Phys. Rev. A* 27, 608, (1983)
- Nellis W.J., Holmes N.C., Mitchell A.C., Trainor R.J., Governo G.K., Ross M. and Young D.A., *Phys. Rev. Lett.* 53, 1248, (1984)
- Nellis W.J., Mitchell A.C., McCandless P.C., Erskine D.T. and Weir S.T., *Phys. Rev. Lett.* 68, 2937, (1992)
- Polian A., Grimsditch M., *Europhys. Lett.* 2, 849, (1986)
- Ree F.H., in *Simple Molecular Systems at Very High Density*, Edit. Polian A., Loubeyre P. and Boccara N., p. 153 (Plenum 1989)
- Ross M., Ree F.H. and Young D.A., *J. Chem. Phys.* 79, 1487, (1983)
- Ross M., *Rep. Prog. Phys.* 48, 1, (1985)
- Ross M. and Radousky H., in *Simple Molecular Systems at Very High Density*, edit. Polian A., Loubeyre P. and Boccara N., p. 47, (Plenum 1989)
- Ruoff A.L. and Vandenberg C.A., *Phys. Rev. Lett.* 66, 754, (1991)
- Ruoff A.L., Xia H. and Xia Q., *Rev. Sci. Instrum.* 63, 4342, (1992)
- Shimizu H., Brody E.M., Mao H.K. and Bell P.M., *Phys. Rev. Lett.* 47, 128, (1981)
- Silvera I.F., *Rev. Mod. Phys.* 52, 393, (1980)
- Silvera I.F. and Wijngaarden R.J., *Phys. Rev. Lett.* 47, 39, (1981)
- Silvera I.F., Eggert J.H., Goettel K.A. and Lorenzana H.E., in *Molecular Systems under High Pressure*, Edit. Pucci R. and Piccitto G., p. 181, (Noth-Holland 1991a)
- Silvera I.F., in *Frontiers of High Pressure research*, edit. Hochheimer H.D. and Etters R.D., p. 101 (Plenum 1991b)
- Streett W.B., *Astrophys. J.* 186, 1107, (1973)
- Surh M.P., Barbee T.W. III and Mailhot C., *Phys. Rev. Lett.* 70, 4090, (1993)
- van den Bergh L.C., Schouten J. and Trappeniers N.J., *Physica A* 141, 524, (1987)
- van Kranendonk, *Solid Hydrogen* (Plenum, New-York 1985)
- Vos W.L., van Hinsberg M.G. and Schouten J.A., *Phys. Rev. B* 42, 6106, (1990)
- Vos W.L., de Kuyper A., Barrat J.L. and Schouten J.A., *J. Phys.: Condens. Matter* 3, 1613, (1991)
- Vos W.L., Finger L.W., Hemley R.J., Hu J.Z., Mao H.K. and Schouten J.A., *Nature* 358, 46, (1992)
- Weir S.T., Nellis W.J. and Mitchell A.C., *Bull. Am. Phys. Soc.* 38, 1520, (1993)
- Weir S.T., Nellis W.J. and Mitchell A.C., *AIRAPT Proceedings* 1993.
- Wigner E. and Huntington J., *J. Chem. Phys.* 3, 764, (1935)
- Young D.A., McMahan A.K. and Ross M., *Phys. Rev. B* 24, 5119, (1981)
- Young D.A., *Phase Diagrams of the elements*, (University of California Press 1991)
- Zeldovich Y. and Raizer Y., *Physics of shock-waves and high temperature hydrodynamic phenomena*, vol. 1 and vol. 2, (New-York, Academic Press 1966)
- Zha C.S., Duffy T.S., Mao H.K. and Hemley R.J., *Bull. Am. Phys. Soc.* 38, 1483, (1993)